Study of Atrato river plume in a tropical estuary: Effects of the wind and tidal regime on the Gulf of Uraba, Colombia

Luis Javier Montoya [a], Francisco Mauricio Toro-Botero [b] & Andrés Gomez-Giraldo [b]

[a] Universidad de Medellin, Medellin, Colombia. ljmontoya@udem.edu.co
[b] Facultad de Minas, Universidad Nacional de Colombia, Medellin, Colombia.fmtoro@unal.edu.co, eagomezgi@unal.edu.co

Abstract
This study focuses on the relative importance of the forcing agents of Atrato River plume as it propagates in a tropical estuary located in the Gulf of Uraba in the Colombian Caribbean Sea. Six campaigns of intensive field data collection were carried out from 2004 to 2007 to identify the main features of the plume and to calibrate and validate a numerical model. Field data and numerical models revealed high spatial and temporal plume variability according to the magnitudes of river discharges, tidal cycles, and wind stress. Atrato River discharge spreads over a considerable portion of the gulf, but only occupies the top 2 m of the surface layer. The tide modifies the position of the plume by inducing a horizontal migration of the salinity front during the day. Two principal modes of circulation in the gulf were identified under different wind conditions.

Keywords: Hydrodynamics; freshwater river plume; tropical estuaries; Gulf of Uraba; ELCOM model.

Estudio de la pluma del río Atrato en un estuario en el trópico: Efectos del viento y del régimen de mareas en el Golfo de Urabá, Colombia

Resumen
Este estudio se enfoca en la evaluación de la importancia de los diferentes forzamientos sobre la pluma del río Atrato y su propagación en un estuario localizado en el golfo de Uraba en el Caribe Colombiano. Se realizaron seis campañas de medición entre los años 2004 y 2007 para identificar las principales características de esta pluma y para la calibración y validación del modelo numérico. Datos de campo y resultados de un modelo numérico muestran que existe una alta variabilidad espacial y temporal en la pluma de acuerdo a la magnitud de la descarga del río, el ciclo de marea y el esfuerzo cortante inducido por el viento. La descarga del río Atrato se dispersa sobre una porción considerable del golfo de Uraba pero ocupa solamente una capa superficial de alrededor de 2 m. La marea modifica la posición de la pluma a lo largo del día, induciendo una migración horizontal en el frente salino. Se identificaron dos modos de circulación en el golfo de Uraba bajo diferentes condiciones de viento.

Palabras clave: Hidrodinámica; plumas estuarinas; estuarios; golfo de Urabá; modelo ELCOM.

1. Introduction

Shelf zone hydrodynamics result from the interaction of several factors such as bathymetry, wind field, freshwater discharges, tides, and the effects of the Earth´s rotation and of oceanic and climatic conditions that affect all the physical chemical biological processes which occur in water. Oceanic circulation at shelf zones influenced by freshwater discharges is radically different from circulation in other oceanic zones because river and shelf currents interact and generate a complex circulation pattern with strong density gradients and localized intensive mixing. When a shelf system has a

significant freshwater discharge input, a region of freshwater influence is formed. For this region, density difference gives rise to strong stratification with a turbid plume front [1]. The shape and extension of these fronts, typically covering only a few meters below the free surface, are variable and depend on river discharges, tidal regimes, the Coriolis effect, and the wind [2]. The dynamics of these fronts are also modified by surface density gradients, friction between layers, and entrainment processes [1]. Stratification is a fundamental process in the control of the vertical structure of the plumes, and because of their proximity to the free surface, movement is controlled by the wind [3, 4].

Studying these zones has several important consequences. Rivers constitute the main source of nutrient-pollutant interchange between continents and oceans, and freshwater plumes have important effects on marine ecosystems. Plumes may become zones of very high biological production. Plume fronts are also important to transport phytoplankton, zooplankton, larvae [5] and nutrients [6], and this has an important impact on shelf environment [6]. These dispersion patterns are directly related to plume dispersion patterns.

Near-shore plume characteristics are functions of a river's different properties as discharge and mouth width, the Coriolis force, shelf slope, wind field, and density differences between water masses. Simpson [7] analyzed a series of physical process in a region of freshwater influence, and topographical effects stood out over the extension and the shape of the plume. This case illustrates situations in which the shape of the coast line controls plume circulation. Semi-enclosed zones are particular cases of these situations, so they follow a special circulation pattern that is significantly modified by bathymetry [8, 9]. In addition, plume evolution time is characterized by complex stratification and mixing patterns [10] that can change quickly in response to tides, winds or river discharges and can be affected by wave-current interaction [11].

Numerical models have been extensively used as a tool to study the hydrodynamics of estuarine fronts [3,12,13] or to analyze real cases [14-18]. Most of the modeling efforts focus on an adequate description of plume dynamics and all previous studies agree that winds [2-4] and tides [16] have an important role in plume dispersion, and that if there are no significant topographic restrictions, the plume turns and spreads parallel to the coast as a result of the Coriolis force. However, most of the studies were conducted at mid latitudes, and there are very few studies for tropical zones [19]. Plumes in tropical zones may behave differently because of many rivers' large freshwater discharges and the weak effect of the Coriolis force. For instance, Nikiema et al. [19] studied Amazon River plume dynamics using a three-dimensional hydrodynamic numerical model to characterize some of the physical processes as a freshwater river discharge on the Amazon River plume with a weak effect of the Coriolis force. Also, there are a few studies of inland seas such as the Caribbean Sea in zones with a micro-tidal regimen and in semi-enclosed regions.

This paper presents the study of Atrato River plume in the Gulf of Uraba, a region near the Equator with a micro-tidal regime in a semi-enclosed zone. These conditions have not been widely studied before and present particular circulation characteristics to give an insight into the most important forcing agents ruling the dynamics of estuaries in the tropics. The hydrodynamics of the Gulf of Uraba was analyzed using a calibrated validated numerical model. Several simulation scenarios were set up to study # circulation patterns under different forcing conditions such as wind fields, tide regimes and Atrato River discharges.

2. The gulf of Uraba

The Gulf of Uraba is a semi-enclosed body of water located in a south-north direction in the Colombian Caribbean Sea near the Colombia-Panama border. The Gulf is located between 7° 55' N and 8° 40' N and between 76° 53' W and 77° 23' (Fig. 1) and is approximately 80-km long with a mean width of 25 km. In the central zone, Atrato River discharge created a typical fluvial delta mainly heading west-east.

Previous studies on the physical oceanography of the Gulf of Uraba [20-24] only analyzed particular conditions and did not identify the importance of forcing agents on the variability of their dynamics in the physical oceanography of the zone.

2.1. Forcing variables

The main driving forces that affect the dynamics of an estuarine front are winds, tides, the Earth's rotation and river discharges [2]. The Atrato River generates a river discharge estimated between 2500 m³/s during the dry season and 5000 m³/s during the rainy season [23]. The wind pattern in the region is affected by the position of an inter tropical convergence zone, and there are two well defined seasons, a dry season from December to March with north and northwesterly winds, and a rainy season from May to November with winds blowing south and southwest. Tides exhibit a semidiurnal pattern with amplitudes of less than 40
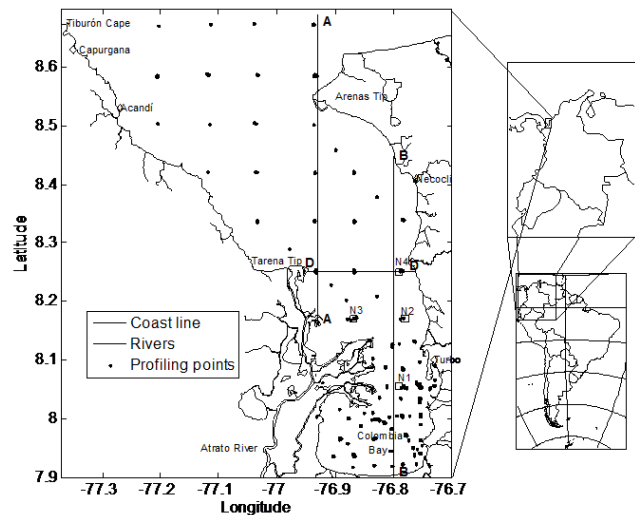

Figure 1. Location of Gulf of Uraba
Source: The authors.

cm [25 and with five dominant astronomical constituents (Mf, O1, K1, M2 and others with low frequency) identified using surface level registers of a tide gauge in San Cristobal, Panama (located at 9° 21' N and 79° 54' W).

3. Materials and methods

3.1. Observational data

Two types of measuring campaigns were conducted for this study. They were general campaigns that included the entire Gulf, and local campaigns that included only the southern zone of the Gulf, Colombia Bay. Three intensive measuring campaigns were carried out in the entire Gulf collecting data from 117 stations using a mini Sea-Bird conductivity temperature depth (CTD) profiler. Three local campaigns were conducted taking salinity and temperature profiles using an IQ net system 2020 XT probe. These campaigns exhibited different wind, tide and river discharge conditions (as shown in Table 1). The locations of the measurement stations are shown in Fig. 1.

Field data revealed that four zones can be identified in the Gulf of Uraba according to stratification patterns: 1) an oceanic zone, 2) a far field plume zone, 3) a near field plume, and 4) Colombia Bay zone (with a variable pattern according to wind direction). Plume thickness ranges from 2 to 4 m (in the far plume, the near field plume and Colombia Bay), and it shows a defined pattern of a highly stratified estuarine front with salinity differences ranging from 7 to 35 in the central zone and from 20 to 35 in the northeastern zone. Also, field data showed that salinity in the plume can vary considerably in time from 15 to 30 in some stations near the plume front. Furthermore, the data showed that the freshwater the river discharged formed a river plume that was maintained near the surface flowing northeast leaving the Gulf parallel to the eastern coast near Punta Arenas in the north-eastern end of the gulf. The surface layer has most of the salinity and the most temperature variations, while the deep layer is homogeneous.

3.2. The numerical model

Field campaign data were used to calibrate and validate the hydrodynamic Estuary, Lake, and Coastal Ocean model (ELCOM), which simulates free-surface flows in lakes and estuaries. ELCOM was developed by the Centre for Water Research (CWR) of the University of Western Australia. It uses hydrodynamic and thermodynamic equations to simulate spatial and temporal variations of velocity, water levels, temperatures, salinity and water density, especially, for stratified bodies of water subjected to environmental forces. ELCOM solves the Reynolds-averaged Navier- Stokes and

Table 1.
Mean Atrato River discharge during measured campaigns

Campaign	Date	Discharge (m³/s)
1	27th - 29th of Oct., 2004	4782.17
2	5th - 8th of June, 2005	3782.54
3	14th - 19th of June, 2006	3803.93
4	19th - 25th of August, 2006	4521.29
5	21th - 24th of Nov., 2006	4782.17
6	12th - 15th of June, 2007	3803.93

Source: The authors.

transport equations using Boussinesq and hydrostatic approximations using an eddy viscosity approximation for horizontal turbulence and a one-dimensional mixed-layer model for vertical Reynolds stress terms [26]. Free surface levels are computed using the vertical integration of the mass conservation equation. To numerically solve these equations, the model uses a semi-implicit method with quadratic Euler-Lagrange discretization of the momentum advection terms [27], the ULTIMATE QUICKEST scheme for scalar transport [28].

4. Results

After a detailed process of calibration and validation [23], ELCOM was used to conduct several numerical experiments to evaluate the effects of the Coriolis force, tides, river discharges and wind fields on the behavior of Atrato River plume. Each forcing factor was changed separately, and the results were compared.

4.1. Calibration and validation

A set of numerical experiments with different grid size and time step were used to compare the performance of the model to numerical parameters allowing the identification of grid size and time step [23]. A horizontal grid of 500 m × 500 m and a non-uniform 33-layer vertical distribution was used. ELCOM is unconditionally stable for pure barotropic flows, but presents stability restrictions associated with the baroclinic term, and discretization appears in stratified flows [26] limiting the time step. Therefore, a time step of 112.5 s was used. The simulation time used was 1 month for all of the simulations where only the last days (between 3 and 7, see Table 1) were used for the analysis. The first days were used to allow the plume to develop and the adjustment of initial conditions.

Data from the first campaign were used for calibration, and the data from the other campaigns were used for validation. Several parameters were adjusted one by one comparing the results of a set of numerical experiments with field data at measuring stations. These parameters were adjusted within physical ranges reported by other authors, and the values of the parameter that offers the best adjustment to the measurements were chosen (for mayor details see [23]). The coefficients and variables chosen for calibration were a mixing model, a diffusion coefficient, percentages of distribution of the discharges by each mouth of the Atrato River and a light extinction coefficient (for more details see [23]). To adjust the model to initial conditions, approximated meteorological data were used such as solar radiation, cloud cover and air temperature obtained from NCEP/NCAR Reanalysis Project data [29]. The wind field was measured in a meteorological station located near the shore in city of Turbo. Small river discharges were estimated using hydrologic balance models [30]. Other values used to represent boundary conditions or physical parameters were a 100 m²/s diffusion coefficient of and a light extinction coefficient of 3.

For all the simulations, a salinity of 35 and a temperature of 30 °C was imposed at the open boundary of the Caribbean

Sea, and a salinity of 10 and a temperature of 27 °C was imposed at river boundaries. The initial condition was obtained by interpolation of measured profiles.

4.1.1. Comparison of field data and model results

During the calibration process, measured and simulated salinity and temperature profiles for the first campaign were compared finding good adjustment with a global root mean square value of 1.29 for the error in salinity and 0.27 °C for the error in temperature, and a correlation coefficient of 0.92 for an adjustment between measured and simulated profiles. These profiles exhibited a good fit, particularly below 4 m of depth with salinity close to 36 and with the major differences found near the surface layers. Greater differences appeared in stations located in the south of Colombia bay. Stations located in the central region of the Gulf and to the north exhibited an adequate fit with differences in the halocline position of less than 40 cm. Temperature profiles exhibited a good fit between simulated and measured profiles, with the larger differences near the surface, and a simulated temperature that was higher than that measured at some stations. It was possibly because of an inaccurate estimate of the light extinction coefficient for these zones, and the deep layers (under 4 m) exhibited a good fit in the entire Gulf.

A comparison of simulated and measured profiles for campaign 1 is presented in Fig. 2, and similar results were found for other campaigns. Generally, good agreement between field measurements and model simulations was found despite some differences. This was so, especially, near the surface in the region near the Atrato river mouth where the model over predicted the measured values. The main differences were found in salinity profiles in the stations located in Colombia Bay. However, a very good fit was found at stations located in the northeast where there is a strong influence of Atrato River plume.

Measurements and field data revealed the river's influence near the surface. During the validation, the RMS of salinity differences ranged from 5.5 to 1.43, and the RMS for temperature differences ranged from 1.62 °C to 0.47 °C.

4.2. Sensitivity analysis. Driving forces

A systematic analysis was performed to study the response of a system to different driving forces and the relative importance of each driving force. Various forcing factors were successively introduced (see results in Fig. 3) into the model to simulate their influence upon the plume. First, simulations were considered with and without Coriolis force. Second, variations in the freshwater discharges were considered, and third, tides and their periodical effect were studied. Finally, the effects of the winds were introduced considering main direction changes which were the main characteristics of the climatic seasons.

4.2.1. Effect of the earth's rotation

At high and mid latitudes, the Coriolis force produces important effects on plume dynamics and distribution that can be
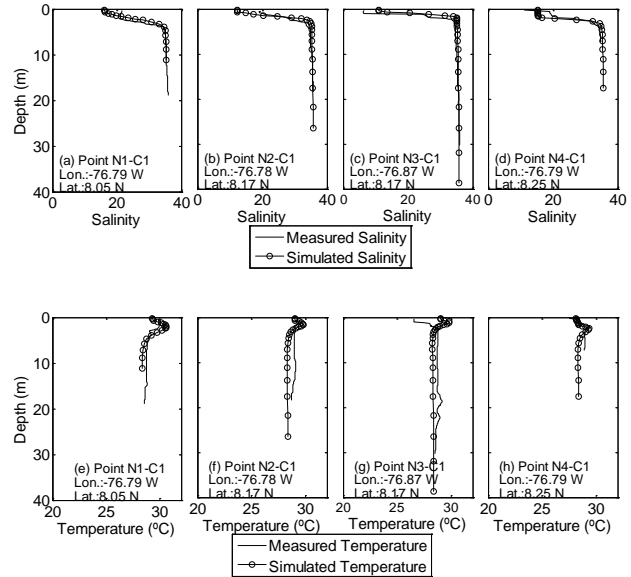

Figure 2. Measured and simulated salinity and temperature profiles in campaign 1.
Source: The authors.

detected from the direction of plume propagation. The plume turns right (in the northern hemisphere) in the absence of other strong forcing factors. The studied zone is located between 7.9° N and 9.4°N latitude; therefore, a moderate Coriolis force effect was expected. Small differences were found comparing results with and without Coriolis acceleration (Figs. 3a, and 3b). However, despite the low value of the Coriolis parameter, its effect must be considered along with the other factors. A simulation considering the Coriolis force (Fig. 3a) produces a plume that leans more towards the northeast coast and with a wider plume slightly lower than simulations without the Coriolis force (Fig. 3b).

4.2.2. Freshwater discharge effect

River discharges affect local plume circulation patterns [2,31], especially, in the near field, where the river's discharge generates an important advection force. A comparison of the simulations for rainy and dry season discharges was conducted (Figs. 4a and 4b), and the results showed that the extension of the plume increases during the rainy season (Fig. 4a) when discharges are higher.

4.2.3. Tidal forcing

Tides play an important role in the mixing process in river plumes. Several authors [19] highlight tide effects on a plume's characteristics analyzing Amazon river plume and reporting the variation in the stratification pattern during tidal cycles while observing periodical movements of a freshwater plume front during the ebb or the flood tide. To introduce tide effects in the simulations, a set of numerical experiments were conducted with different tide forcing with tide forcing estimated using 5 of the principal harmonics (Fig. 3a) and with no tide at all (Fig. 5).
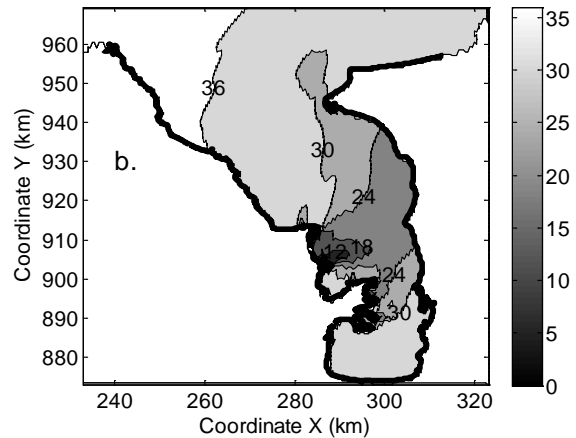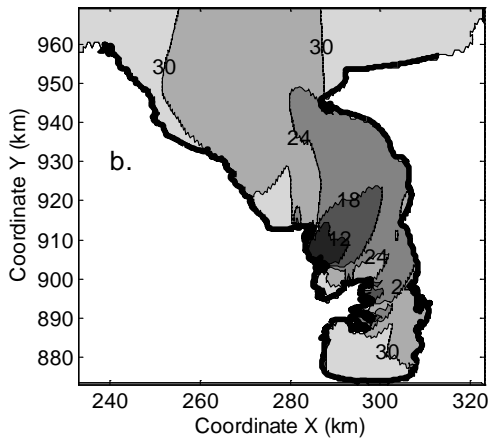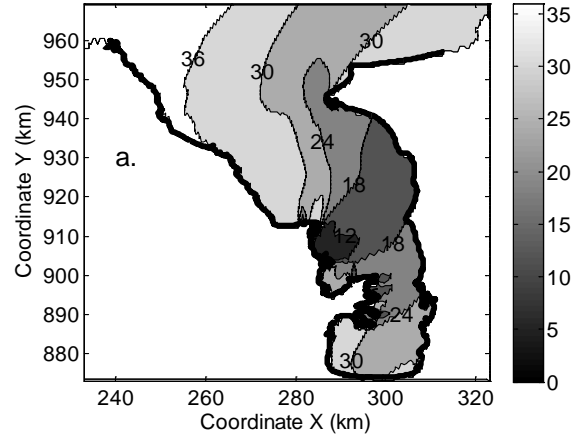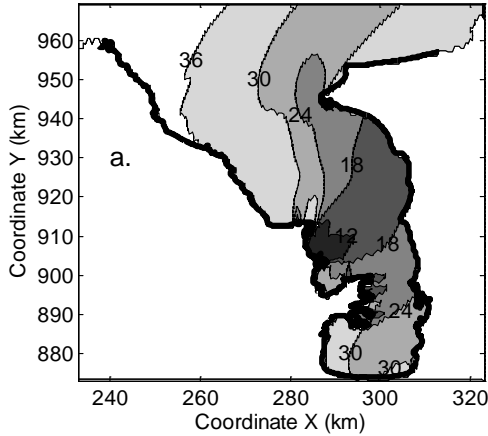
Figure 3. Mean surface salinity for different simulation conditions with 2.3 m/s SW winds. (a) Considering Coriolis effect (b) Not considering Coriolis effect. Source: The authors.

Figure 4. Mean surface salinity for different simulation conditions with 2.3 m/s SW wind. (a) High river discharge (b) Low river discharge. Source: The authors.

4.2.4. Wind effects

Different authors pointed out that the wind plays an important role in the circulation of an estuarine plume [3], and reported different plume responses according to wind direction [2]. There are variations in the thickness, width, and propagation speed of a plume in response to wind stress changes [34]. Wind forcing has a strong influence on the characteristics of a buoyant plume because the momentum added by wind stress is trapped in a relatively thin layer which has a low level interchange with the oceanic layer because of density differences [34]. Winds induce a shear stress on the surface layer that can act in favor of or against the buoyant plume motion, promoting or hindering plume dispersion. Lentz and Lagnier [34] show three situations of buoyant plume response to different along-shelf wind forcing: (a) upwelling wind promoting plume spread causing plume to become thin and wide, (b) moderate downwelling wind, inhibiting plume development and causing a thicker narrower plume with a steep front, and (c) strong downwelling winds causing vertical mixing. Simple models had been used to try to explain the response to upwelling winds [4]. However, there is no general model that provides quantitative estimates of the dependence of plume characteristics on wind stress.
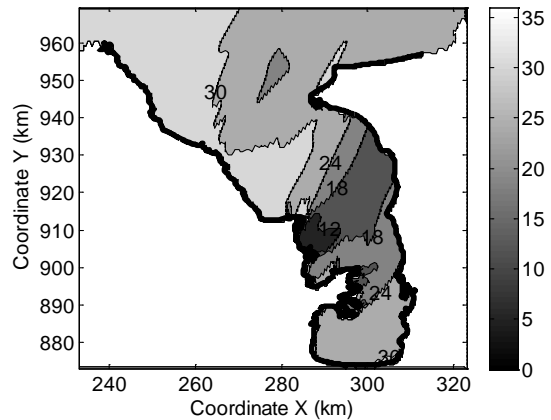

Figure 5. Mean surface salinity with 2.3 m/s SW wind and non-tide. Source: The authors.

Figs. 6a and 6b show the results of two simulation cases with different wind patterns. The shape and direction of the plume was particularly sensitive to wind direction. Northerly winds (Fig. 6b) direct the plume South increasing plume surface mixing. On the other hand, southerly winds (Fig. 3a),
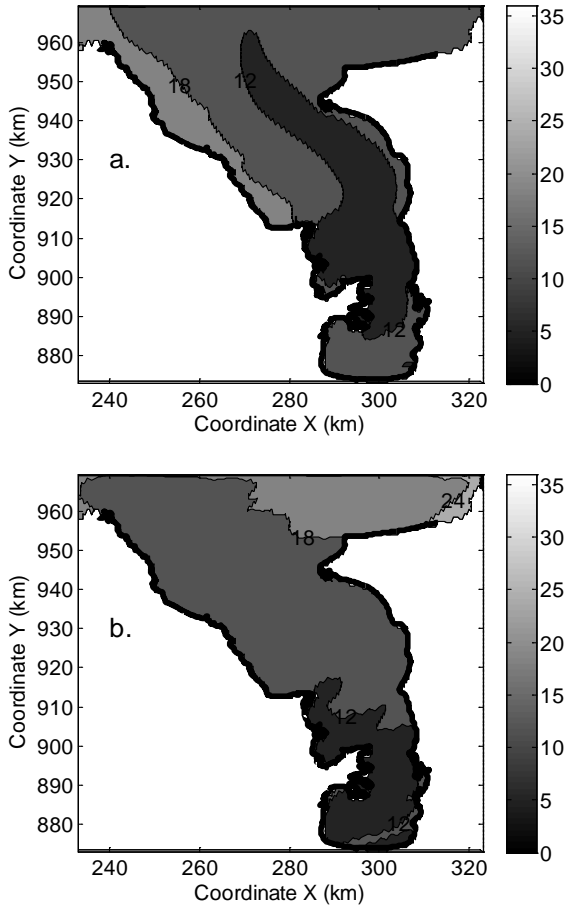
Figure 6. Mean Surface salinity for different simulation conditions. (a) no-wind (b) NW wind.
Source: The authors.

Figure 7. Surface salinity and velocity during (a) ebb tide and (b) flood tide in campaign 3.
Source: The authors.

direct the plume northwards forcing the plume to leave the gulf by the northeast coast generating a surface plume. No-wind conditions, (see Fig. 6a) allow mixing near the surface by the tidal effect. All the simulation cases show that wind effects were limited to the surface layer. A comparison of the vertical structure of water for different wind scenarios showed that waters deeper than 4 m are practically the same. Two distinct circulation plume patterns were found. One had a southwest-northeast direction induced by southwest winds, and a second pattern induced by northeast winds which guided the plume southwards. Wind direction affects plume direction and imposes a direction that can be intensified or decreased by other factors such as tides or river discharges [23].

4.3. Plume dynamics

Surface circulation is strongly influenced by Atrato River plume. To analyze surface currents in the Gulf of Urabá, Figs. 7a and 7b show velocity and surface salinity (on June 18, 2006 at 6:00 a.m. (a) and 6:00 p.m. (b). They were obtained with simulations of the climatic conditions during campaign 3 at ebb and flood tides (Fig. 7g) with southeast winds (uniform over the whole domain, with the magnitude and direction shown in Figs. 7e and 7f). The vertical structure of
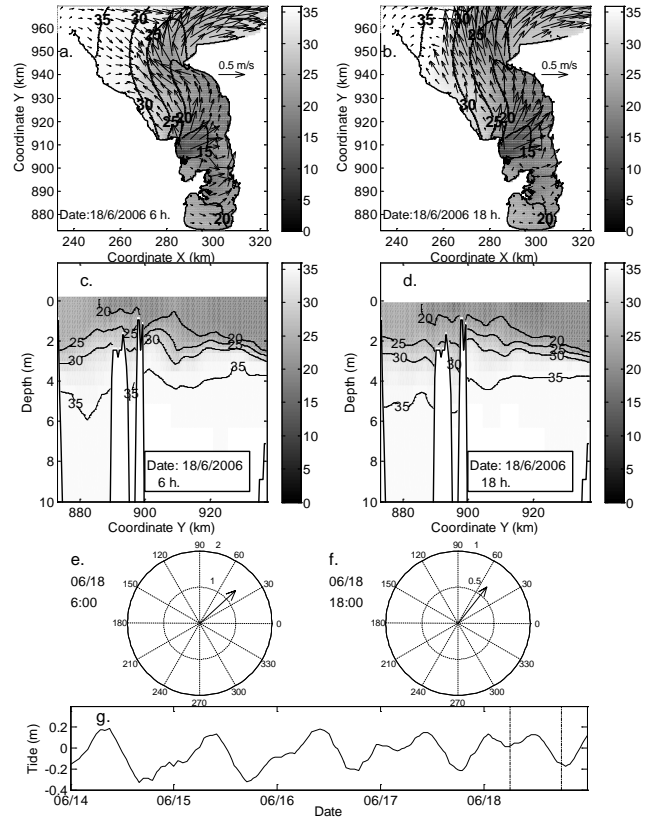
salinity in the plume is presented for previous conditions in Figs. 7c and 7d along section A-A (see location in Fig. 1). A comparison of surface salinity contours (Figs. 7a and 7b) shows tide-related variations throughout the day, especially, near the river mouth.

The plume spreads from the river mouth and heads east driven by river advection. When the plume reaches the east coast, it turns left heading north forming a coastal current leaving the gulf via the northeast coast, and finally, it turns east as a coastal current outside the gulf. This behavior was found with different intensities in all the campaigns. A general analysis of the simulated characteristics showed four horizontal zones in the Gulf which were: (1) an oceanic influenced zone in the northwest with homogenous salinity and temperature profiles (salinity from 30 to 36 and temperatures from 28 to 30 °C), (2) a region of freshwater influence characterized by a strong stratification around 2 m (salinity from 7 to 36) with a surface layer occupying the central and northeast portions of the Gulf, which could be divided as near field and far field, (3) a region to the south in Colombia Bay with salinity variations ranging from 15 to 36 and high spatial variability in the stratification, and (4) an oceanic water mass that occupies the deepest layer (under 4 m of depth) covering the entire gulf.

Fig. 8 shows a detail of section B-B near the river mouth at different times of June 6 and 7, 2005. The zonal velocity along section B-B is greater near the surface layer, and
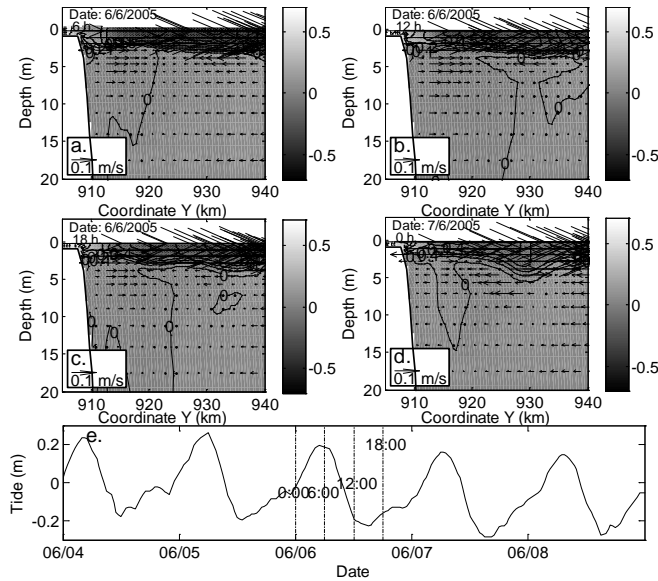
Figure 8. Zonal velocity along the longitudinal axis (section B–B) at different times during campaign 2.
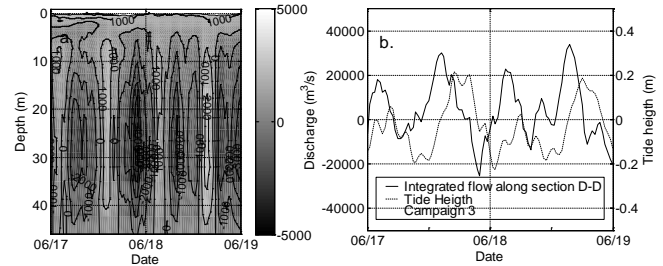Source: The authors.

Figure 9. Width integrated discharge and total discharge along section D-D for two days of campaign 3. (Positive values indicate that the flow is going out of the gulf)
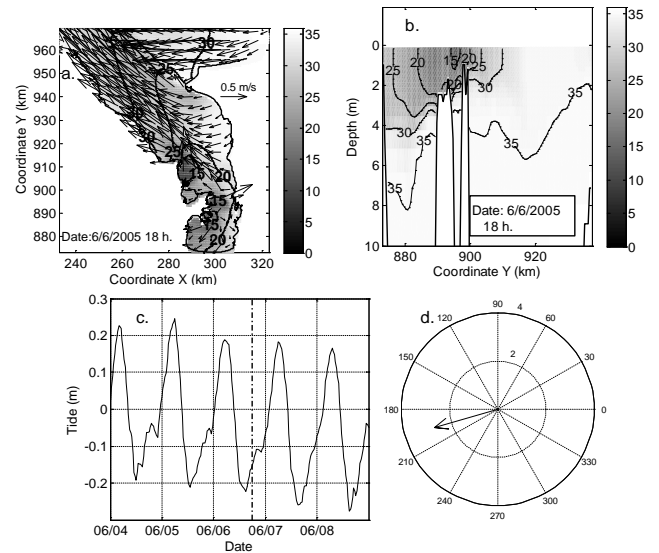Source: The authors.

Figure 10. Surface salinity during northeast wind condition during campaign 2. (a) Surface salinity and velocity (b) Section A-A (c) Tide condition (d) Wind condition.
Source: The authors.

particularly, near the river mouth as a result of the strong advection induced by river discharges. A seaward current in the plume and a net landward current at lower layers reveal a typical estuarine circulation.

Simulation results of other campaigns (not shown) reveal a similar behavior. In section B-B, the maximum velocity is located near the river mouth with approximate values of 0.6 m/s. High values of the zonal velocity were found at the first 2 m of plume depth (Fig. 8) indicating that the plume has a velocity which is greater than the deepest oceanic layer.

The plume exhibits significant velocity reductions below the halocline, and it was not notably affected by wind action. Most of the time, the velocity at surface layer flows out of the gulf, whereas the oceanic layer changes the direction of the velocity throughout the day. During the flood tide (Figs. 8a and 8c), the velocity enters the gulf, and during the ebb tide (Fig. 8d) the velocity leaves the gulf. Typical current speeds are 0.3 m/s in the surface layer and 0.05 m/s in the oceanic layer. At deeper layers, currents (below 2 m) change magnitude and direction during the day. Simulations exhibit plume movement during the day as a result of tidal forcing changing the location of the plume. During the ebb tide, the plume reaches its maximum extension in the Gulf, and during the flood tide, freshwater flow shrinks the plume back.

Regarding mass flux, simulations reveal (Fig. 9) that there was a permanent flow leaving the Gulf (positive discharges) via surface layers and an oscillatory flow below the halocline (below 4 m deep) but with a net flow entering the gulf to compensate the effects of surface flow. Surface flow presents low salinity and relatively strong velocities, and deep flow presents high salinity, low velocity, and changes in direction according to ebb tides and flood tides. The total mass crossing section D-D follows tide oscillation as seen in Fig. 9b although a face lag of roughly 4 hours is also clear.

The wind field modifies the position of the salinity front, which is subject to periodical horizontal migration under tide forcing. For example, Fig. 10 shows surface salinity and a vertical cross section A-A during campaign 2. The Northeast winds (Figs. 10a and 10b) have an important effect on plume extension, deflecting and spreading it towards the northwest. From south to north, Fig. 10b shows the salinity along section A-A, and it is clear that the plume remains near the surface in the region near the river mouth (coordinate 900 km in Fig. 10a). As one moves north, salinity increases towards oceanic values indicating that plume influence is no longer active in this region: it has moved to a northwesterly direction.

5. Discussion

5.1. Characteristics of plume motion

Studies of Rhone river plume [15,31], Ebro river plume [32], Columbia river plume [17], and Río de la Plata river plume [2] revealed that the Coriolis force is fundamental in plume motion, particularly its deflection along the coast. However, studies of river plumes near the Equator, like

Amazon River plume [19] show that coastal currents have a fundamental role in plume dynamics. When a river discharge occurs in semi-enclosed zones like a bay or a gulf, residual baroclinic flows can appear [8, 9] as a response to topographic forcing. Near the Equator, plume dynamics are controlled by winds, tides, and river discharges and, less importantly, by the Coriolis force. In the Gulf of Uraba, we found that wind direction rules surface circulation and that tides play a role on plume motion by enhancing it during ebb tides, and constraining its spread during flood tides. The currents below the halocline are governed completely by the tidal force.

Atrato River plume has the characteristic properties of a low-latitude plume generated by a high river discharge. According to Garvine's [12] classification of dynamics, Atrato River plume with a Kelvin number of 0.56 should be classified as a "small-scale" discharge. Its low Kelvin number value appears because of the effect of its low latitude where the Rosby radius is long. This means that near the Equator, plumes have an important contribution from all momentum terms as advection, pressure gradient, wind stress and basal current stress [19]. According to Yankovsky and Chapman [33], Atrato River plume would be classified as intermediate in behavior. However, its structure reveals a surface-advected plume behavior. It is also necessary to bear in mind the topographic restriction imposed on the plume for the Gulf of Uraba coastline making it turn north.

For a better understanding of these plume dynamics, they can be described in terms of water masses. Near the river mouth, strong non-linear dynamics can be observed. A strong advection dominates plume motion, and plume behavior is a jet-like outflow dominated by the momentum of the river (close to the mouth). In the far field, far away from the river mouth, plume distribution changes according to wind direction in such a way that even low wind magnitudes can affect plume dynamics. The intensity of the mixing processes in this plume zone is modified by tides, winds and river discharges. Baroclinic flow was evident from the persistent flow that leaves the gulf via the northeast coast caused by a pronounced salinity gradient. This baroclinic flow appears only in the surface layer, but the entrainment induced a mixing process in the plume, and an opposite flow was required in the deeper layers to compensate for the flow entrainment in the plume. Barotropic tide-induced movements are detected for the region below the plume, specifically, below 2 m deep. A tidal current generates basal stress, and during the ebb tide the current goes out of the gulf and propitiates plume movement. While during flood tide, the current enters the gulf making it more difficult for the plume to spread.

Finally, as in other studies [5,2], numerical models and field observations have shown that wind forcing has a strong influence on the plume's characteristics. Atrato River plume simulations show that under different wind forcing conditions, wind stress is an important factor of plume structure. According to wind direction, wind stress makes it either difficult or easy for a plume to move. A wind-induced momentum flux is trapped in a relatively thin plume and strong stratification hinders wind momentum transference to the deepest layers. An important relationship between wind direction and shape and plume extension were found in the Gulf of Uraba. Southeast winds and currents during ebb tide facilitated plume movement while northeast winds directed the plume south and brought about plume mixing. Thus, we can conclude that both of these forcing factors affect the plume, and they can have a common effect when the plume heads Northeast.

6. Summary and conclusions

Atrato River plume dynamics in the Gulf of Uraba were studied using field data and numerical modeling. Field measurements and numerical simulation show a strong saline stratification in the Gulf. This stratification is explained by the Atrato River's high discharges into the Gulf. Both, observation and numerical simulations reveal that the highest vertical salinity gradients are near the surface below the river's water layer with a thickness of less than 2 m. Gulf of Uraba hydrodynamics are the result of the combined action of tides, winds, and the Atrato river's discharge. The Coriolis force produces a plume that leans more towards the northeast coast. Freshwater discharge affects the extension of the plume. Plume extension is increased during the rainy season with high river discharge. The combined action of tides and winds strongly influence the extension of the plume and its structure. Ebb tides bring about the formation and development of a surface plume with currents leaving the gulf that may be enhanced by the wind field in favorable conditions. On the other hand, flood tides hinder the development of the plume which is affected by wind action making it spread or constrain depending on whether or not the wind blows in the direction of plume movement. Regarding wind effects, simulation results suggest two different plume behaviors. One has the plume heading southwest to northeast induced by southwestern winds, and the second has the plume heading southwards when winds blow from the northwest.

Acknowledgements

References

[1] Bowman, M.J., Estuarine fronts, in hydrodynamics of estuaries. Volume I: Estuarine Physics, Boca Raton, FLA: CRC press, 1988, pp. 86-131.

[2] Simionato, C.G., Dragani, W., Meccia, V. and Nuñez, M., A numerical study of the barotropic circulation of the Río de la Plata estuary: sensitivity to bathymetry, the Earth's rotation and low frequency wind variability. Estuarine, Coastal and Shelf Science, 61, pp. 261-273, 2004. DOI: 10.1016/j.ecss.2004.05.005

[3] Chao, S.Y., Wind-driven motion of estuarine plumes. Journal of Physical Oceanography, 18, pp. 1144-1166, 1988. DOI: 10.1175/1520-0485(1988)018<1144:WDMOEP>2.0.CO;2

[4] Fong, D.A. and Geyer, W.R., Response of a river plume during an upwelling favourable wind event. Journal of Geophysical Research, 106, pp. 1067-1084, 2001. DOI: 10.1029/2000JC900134

[5] Garcia-Berdeal, I., Hickey, B. and Kawase, M., Influence of wind stress and ambient flow on a high discharge River Plume. Journal of Geophysical Research – Oceans, 107(C9), pp. 13_1-13_24, 2002.

DOI: 10.1029/2001JC000932

[6] Spillman, C.M., Imberger, J., Hamilton, D.P. Hipsey, M.R. and Romero, J.R., Modelling the effects of Po River discharge, internal nutrient cycling and hydrodynamics on biogeochemistry of the Northern Adriatic Sea. Journal of Marine Systems, 68, pp. 167-200, 2007. DOI: 10.1016/j.jmarsys.2006.11.006

[7] ¿Simpson, J.H., Physical processes in the ROFI regime. Journal of Marine Systems, 12, pp. 3-15, 1997. DOI: 10.1016/S0924-7963(96)00085-1

[8] Fujiwara, T., Sanford, L.P., Nakatsuji, K. and Sugiyama, Y., Anti-cyclonic circulation driven by the estuarine circulation in a gulf type ROFI. Journal of Marine System, 12, pp. 83-99, 1997. DOI: 10.1016/S0924-7963(96)00090-5

[9] James, I.D., A numerical model of the development of anticyclonic circulation in a gulf-type region of freshwater influence. Continental Shelf Research, 17(14), pp. 1803-1816, 1997. DOI: 10.1016/S0278-4343(97)00052-6

[10] Hetland, R.D., Relating river plume structure to vertical mixing. Journal of Physical Oceanography, 35(9), pp. 1667-1688, 2005. DOI: 10.1175/JPO2774.1

[11] Rong, Z., Hetland, R.D., Zhang, W. and Zhang, X., Current-wave interaction in the Mississippi-Atchafalaya river plume on the Texas-Louisiana shelf. Ocean Modelling, 84, pp. 67-83, 2014. DOI: 10.1016/j.ocemod.2014.09.008

[12] Wiseman, W. and Garvine, R., Plumes and coastal currents near large river mouths. Estuaries, 16(3), pp. 22 509-517, 1995.

[13] Garvine, R., A dynamical system for classifying buoyant coastal discharges. Continental Shelf Research, 15, pp. 1585-1596, 1995. DOI: 10.1016/0278-4343(94)00065-U

[14] Estournel, C., Broche, P. Marsaleix, P. Devenon, J.L. Auclair, F. and Vehil, R., The Rhone River plume in unsteady conditions: Numerical and experimental results. Estuarine, Coastal and Shelf Science, 53, pp. 25-38, 2001. DOI: 10.1006/ecss.2000.0685

[15] Tilburg, C.E. and Garvine, R.W., Three-dimensional flow in a Shallow Coastal upwelling zone: Alongshore convergence and divergence on the New Jersey shelf. Journal of Physical Oceanography, 33, pp. 2113-2125, 2003. DOI: 10.1175/1520-0485(2003)033<2113:TFIASC>2.0.CO;2

[16] Whitney, M. and Garvine, R., Simulationg the Delaware Bay Bouyant outflow: Comparison with observations. Journal of Physical Oceanography, 36, pp. 3-21, 2006. DOI: 10.1175/JPO2805.1

[17] Baptista, A., Zhang, Y., Chawla, A., Zulauf, M., Seaton, C., Edward, P., Myers, E. P., Kindle, J., Wilkina, M., Burla, M. and Turner, P., A cross-scale model for 3D baroclinic circulation in estuary–plume–shelf systems: II. Application to the Columbia River. Continental Shelf Research, 25, pp. 935-972, 2005. DOI: 10.1016/j.csr.2004.12.003

[18] Farcieri, F.M., Benetazzo, A., Sclavo, M., Russo, A. and Carniel, S., Po River plume pattern variability investigated from model data. Continental Shelf Research, 87, pp. 84-95, 2014. DOI: 10.1016/j.csr.2013.11.001

[19] Nikiema, O., Devenon, J.-L. and Baklouti, M., Numerical modeling of the Amazon River plume. Continental Shelf Research, 27, pp. 873-899, 2007. DOI: 0.1016/j.csr.2006.12.004

[20] Chevillot, P., Molina, A. Giraldo, L. y Molina, C., Estudio geológico e hidrológico del golfo de Urabá. Boletín Científico CIOH, 14, pp. 79-89, 1993.

[21] Bernal, G., Montoya, L.J., Garizabal, C. y Toro, M., La complejidad de la dimensión física en la problemática costera del Golfo de Urabá, Colombia. Gestión y Ambiente, 8, pp. 123-135, 2005.

[22] Lonin, S. y Vásquez, J., Hidrodinámica y distribución de coliformes en el Golfo de Urabá, Boletín Científico CIOH, 23, pp. 76-89, 2005.

[23] Montoya, L.J. y Toro, M., Calibración de un modelo hidrodinámico para el estudio de los patrones de circulación en el Golfo de Urabá, Colombia. Avances en Recursos Hidráulicos, 13, pp. 37-54, 2006.

[24] Escobar, C.A., Velásquez, L. and Posada, F., Marine currents in the Gulf of Urabá. Colombian Caribbean sea. Journal of Coastal Research, 6, pp. 1363-1374. 2015. DOI: 10.2112/jcoastres-d-14-00186.1

[25] Correa, I.D. y Vernette, G., Introducción al problema de la erosión litoral en Urabá (sector Arboletes-Turbo) Costa Caribe Colombiana. Boletín Investigaciones Marinas y Costeras, 33, pp. 7-28, 2004.

[26] Hodges, B., Imberger, J., Saggio, A. and Winters, K.B., Modeling basin-scale internal waves in strafied lake. Limnology and Oceangraphy, 45(7), pp. 1603-1620, 2000. DOI: 10.4319/lo.2000.45.7.1603

[27] Casulli, V. and Cheng, R.T., Semi-implicit finite difference methods for three-dimensional shallow water flow. International Journal for Numerical Methods in Fluids, 15, pp. 629-648, 1992. DOI: 10.1002/fld.1650150602

[28] Leonard, B.P., The ULTIMATE conservative difference scheme applied to unsteady one-dimensional advection. Computer Methods in Applied Mechanics and Engineering. 88, pp. 17-74, 1991. DOI: 10.1016/0045-7825(91)90232-U

[29] Kalnay, E., Kanamitsu, M., Kistler, R., Collins, W., Deaven, D., Gandin, L., Iredell, M., Saha, S., White, G., Woollen, J., Zhu, Y., Chelliah, M., Ebisuzaki, W., Higgins, W., Janowiak, J., Mo, K,C., Ropelewski, C., Wang, J., Leetmaa, A., Reynolds, R. and Dennis, Joseph, R.J., The NCEP/NCAR 40-Year Reanalysis Project. Bulletin of the American Meteorological Society, 77(3), pp. 437-471, 1996. DOI: 10.1175/1520-0477(1996)077<0437:TNYRP>2.0.CO;2

[30] Poveda, G., Mesa, O.J., Velez, J.I., Mantilla, R., Ramirez, J.M., Hernández, O.O., Borja, A.F. and Urzola, J.A., HidroSIG: An interactive digital atlas of Colombia's hydro-climatology. Journal of Hydroinformatics, 9, pp. 145-156, 2007. DOI: 10.2166/hydro.2007.009

[31] Ulses, C., Grenz, C., Marsaleix, P., Schaaff, E., Estournel, C., Meule, S. and Pinazo, C., Circulation in a semi-enclosed bay under influence of strong freshwater input. Journal of Marine Systems, 56, pp. 113-132, 2005. DOI: 10.1016/j.jmarsys.2005.02.001

[32] Sierra, J.P., Sanchez-Arcilla, A., Del Rio, J.G., Flos, J., Movellan, E., Mosso, C., Martinez, R., Rodilla, M., Falco, S. and Romero, I., Spatial distribution of nutrients in the Ebro estuary and plume, Continental Shelf Research, 22, pp. 361-378, 2002. DOI: 10.1016/S0278-4343(01)00061-9

[33] Yankovsky, A.E. and Chapman, D.C., A simple theory for the fate of bouyant coastal discharge, Journal of Physical Oceanography, 27, pp. 1386-1401, 1997. DOI: 10.1175/1520-0485(1997)027<1386:ASTFTF>2.0.CO;2

[34] Lentz, S.J. and Largier, J., The influence of wind forcing on the Chesapeake Bay buoyant Coastal Current. Journal of Physical Oceanography, 36, pp 1305-1316, 2006. DOI: 10.1175/JPO2909.1

L.J. Montoya, completed his BSc. Eng in Civil Engineering in 1998, the MSc. degree in Water Resources Research in 2001, and the PhD. degree in Engineering in 2009, all of them at Universidad Nacional de Colombia, Medellín, Colombia. Currently, he is a full professor in the School of Engineering at Universidad de Medellin, Colombia. His research interests include hydrodynamics, environmental fluids dynamics and sediment transport.
ORCID: 0000-0002-5832-2219

F.M. Toro-Botero, completed his BSc. Eng in Civil Engineering in 1981 at Universidad Nacional de Colombia, MSc. of Science in Engineering in 1985 and a PhD in Hydroscience and Engineering in 1994 both at the University of Mississippi, USA. Currently, he is a titular professor of the graduate program on Water Resources Management in the Geosciences and Environmental Department, Facultad de Minas, Universidad Nacional de Colombia. He is an active member of PARH and Oceanic research groups. His research interests include numerical methods in hydrodynamics, hydrodynamics, numerical hydrodynamical modelling in coastal areas and inland waters, and water quality modelling.
ORCID: 0000-00018524-2014

A. Gomez-Giraldo, completed his BSc. Eng in Civil Engineering in 1995, MSc. degree in Water Resources Research in 1998 both at Universidad Nacional de Colombia, Medellin, Colombia, and his PhD. degree in Environmental Engineer at the University of Western Australia. Currently, he is an associate professor of the graduate program on Water Resources Management in the Geosciences and Environmental Department at the School of Mines at Universidad Nacional de Colombia. His research interests include physical limnology, tropic limnology, hydrodynamics, environmental fluids dynamics; numerical hydrodynamical modelling in coastal areas and inland waters and water quality modelling.
ORCID: 0000-0001-7103-9429